Full Counting Statistics of Laser Excited Rydberg Aggregates in a One-Dimensional Geometry

H. Schempp,[1] G. Günter,[1] M. Robert-de-Saint-Vincent,[1] C. S. Hofmann,[1] D. Breyel,[2] A. Komnik,[2] D. W. Schönleber,[3] M. Gärttner,[3] J. Evers,[3] S. Whitlock,[1,*] and M. Weidemüller[1,†]

[1]*Physikalisches Institut, Universität Heidelberg, Im Neuenheimer Feld 226, 69120 Heidelberg, Germany*

[2]*Institut für Theoretische Physik, Universität Heidelberg, Philosophenweg 16, 69120 Heidelberg, Germany*

[3]*Max-Planck-Institut für Kernphysik, Saupfercheckweg 1, 69117 Heidelberg, Germany*

(Received 1 August 2013; revised manuscript received 15 October 2013; published 7 January 2014)

We experimentally study the full counting statistics of few-body Rydberg aggregates excited from a quasi-one-dimensional atomic gas. We measure asymmetric excitation spectra and increased second and third order statistical moments of the Rydberg number distribution, from which we determine the average aggregate size. Estimating rates for different excitation processes we conclude that the aggregates grow sequentially around an initial grain. Direct comparison with numerical simulations confirms this conclusion and reveals the presence of liquidlike spatial correlations. Our findings demonstrate the importance of dephasing in strongly correlated Rydberg gases and introduce a way to study spatial correlations in interacting many-body quantum systems without imaging.

DOI: 10.1103/PhysRevLett.112.013002 PACS numbers: 32.80.Rm, 03.65.Yz, 34.20.Cf

Central questions in the physics of strongly correlated many-body systems are what is the nature of the correlations (e.g., quantum versus classical), how do they arise, and how can they be probed in real physical systems [1–6]? Rydberg atoms with their extreme properties and long-range interactions are an ideal system to study strongly correlated regimes, especially since the laser excitation itself in combination with strong interactions naturally produces spatial and temporal correlations [7–15]. One exciting prospect is to deterministically prepare a "quantum crystal" of Rydberg excitations by adiabatically following the ground state of the laser-dressed system [16–19]. However, aside from this very specific preparation scheme, the precise nature of the excitation process is not yet well understood, especially in the presence of dephasing or decoherence. An open question is whether many-body states are created simultaneously in a coherent multiphoton process or if they arise due to sequential excitations of individual atoms around an initial grain. Recently, there has been a lot of theoretical work focusing specifically on low-dimensional systems in which long-range correlations can build up without the need for adiabatic preparation. Both resonant [20–24] and off-resonant [25–30] excitation have been considered, which feature different mechanisms leading to the formation of correlated structures.

Here we report the excitation of strongly correlated structures, which we call Rydberg aggregates, in a quasi-one-dimensional geometry. We make use of the full counting statistics (FCS) of the Rydberg atom number to characterize the many-body system, which serves as a complementary approach to direct imaging of spatial correlations [12,13,31]. So far, experiments on the statistics of Rydberg atoms have mainly analysed reduced number fluctuations due to the dipole blockade effect under close to resonant driving [8,11,14,15]. In contrast, we interpret *enhanced* number fluctuations which we observe for detuned excitation. We introduce a simplified picture to explain the effect of correlations on the FCS. We attribute the enhanced fluctuations to the excitation of Rydberg aggregates comprised of several atoms at well-defined distances. To identify the dominant formation mechanisms we compare the rates for direct multiphoton excitation and sequential excitation in which an initial grain is excited slowly, followed by much faster resonant excitation at preferred distances. Our conclusions are supported by many-body simulations which include the relevant experimental parameters.

In order to get an intuitive understanding of the excitation process we start with a simple picture for how the statistical distribution of Rydberg atoms is influenced by the laser coupling, in particular, as a function of detuning. We consider Rydberg atoms in a one-dimensional geometry with repulsive interactions. Figure 1(a) shows a sketch of the bare energies of the many-body states in the rotating frame. Each energy level decreases linearly with detuning Δ, with the slope proportional to the number of excitations m and the offset equal to the total interaction energy [10,17–19]. The dashed rectangle represents the states that can be excited for a given detuning.

The resonance condition for direct multiphoton excitation is $E = 0$; however, aggregates can also form by an off-resonant excitation at the energy of the $m = 1$ state ($E = -\Delta$), followed by additional resonant excitations. For positive detunings, configurations with positive interaction energy are energetically favored [10,30,32]. Hence, we expect an enhancement of Rydberg excitations for $\Delta > 0$. Independent creation of aggregates is expected

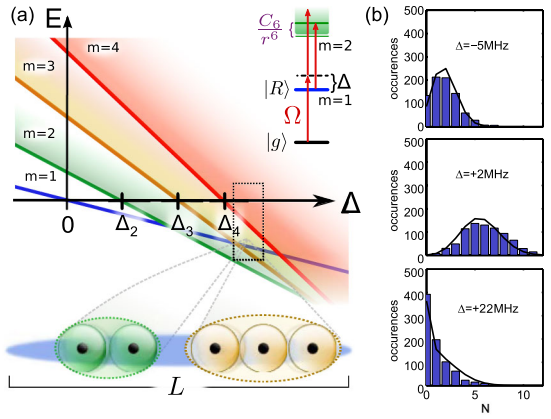

FIG. 1 (color online). (a) Level scheme and many-body energies in a rotating frame for Rydberg aggregates of size m as a function of laser detuning Δ. The shaded areas indicate the manifold of excited states corresponding to different spatial configurations. Zero energy crossings for the lowest energy states occur at $\Delta_m = C_6(m-1)^7/(mL^6)$, where L is the system length and C_6 is the van der Waals interaction strength. For a given detuning and laser dephasing, aggregates of different sizes are formed (dotted rectangle), either through sequential growth or by multiphoton excitation. (b) Measured histograms of the Rydberg atom number distribution for different detunings. The solid lines are the results of the numerical simulations (see text).

in the long-time limit of the fully coherent system [30]. The finite duration of the excitation does not evolve the system into the global steady state, which together with the laser dephasing promotes the formation of different aggregate sizes in different parts of the excitation volume. This bunching of excitations will have a dramatic effect on higher order moments of the statistical distribution. Assuming independent excitation of nearly equally sized aggregates (same m), the variance of the Rydberg number N scales as $\mathrm{var}(N) = m\langle N\rangle$. Higher-order moments of the distribution also scale with simple powers of m (see Supplemental Material [33]). Therefore, the resulting super-Poissonian statistics provide a measure of the typical size of aggregates.

The experiments are carried out as follows. First we prepare approximately 1.5×10^4 ^{87}Rb atoms in the state $|g = 5S_{1/2}, F = 2, m_F = 2\rangle$ in a tightly focused optical dipole trap [34]. This results in an elongated atom cloud with $e^{-1/2}$ radii of $\approx 240\ \mu m \times 1.65\ \mu m$ (axial $\times$ radial). The imaged radial cloud size of 3.5 μm is limited by optical resolution; therefore, we adjust this parameter in comparison with theory. However, it is smaller than the blockade radius which sets a limit on the closest possible distance between Rydberg atoms [35], giving rise to a quasi-1D geometry with respect to the Rydberg excitations. The maximal peak density of ground state atoms is $\approx 1.5 \times 10^{12}$ cm^{-3}, corresponding to a mean interparticle spacing at the trap center of ≈ 0.9 μm. Lower densities are achieved by reducing the time taken for initial loading of the dipole trap.

Rydberg atoms in the state $|R = 50S_{1/2}\rangle$ are excited by applying a two-photon laser pulse for 5 μs (after turning off the optical trap). The lasers are close to two-photon resonance, detuned $\delta = 65$ MHz below the intermediate $|5P_{3/2}, F = 3, m_F = 3\rangle$ state. The first laser at 780 nm uniformly illuminates the cloud, while the second excitation laser at 480 nm is focused to an elliptical region of size $\approx 27\ \mu m \times 11\ \mu m$ (vertical $\times$ horizontal Gaussian beam waists). The two excitation laser beams counterpropagate and cross the atomic cloud perpendicular to its long axis. The effective (single-atom) two-photon Rabi frequency is $\Omega \approx 0.4$ MHz (peak value) and the linewidth related dephasing between the ground and Rydberg state is $\Gamma \approx 1$ MHz. The two-photon detuning Δ can be varied by scanning the second step laser frequency.

The Rydberg atoms interact repulsively with the van der Waals coefficient $C_6 = 16\ \mathrm{GHz}\,\mu\mathrm{m}^6$ [36]. In the low density limit this gives a blockade radius of $R_c \approx 5.3$ μm. At a density of 1.5×10^{12} cm^{-3}, however, we expect $N_{bl} \approx 160$ atoms per blockade sphere. As a result the Rabi frequency is collectively enhanced $\sqrt{N_{bl}}\Omega \approx 5.0$ MHz and, correspondingly, $R_c \approx 4.1$ μm [37]. Given our geometry we anticipate that 10–15 Rydberg excitations are possible. After excitation we field ionize the Rydberg atoms and count the number of ions detected on a microchannel plate (MCP) detector, with an estimated detection efficiency of $\eta \approx 0.4$ [15]. By repeating the experiment several hundred times we build up statistical distributions of the Rydberg number which are observed to have qualitatively different shapes for different detunings [Fig. 1(b)].

Figure 2 shows the measured mean Rydberg atom number $\langle N\rangle$ as a function of the two-photon detuning Δ for

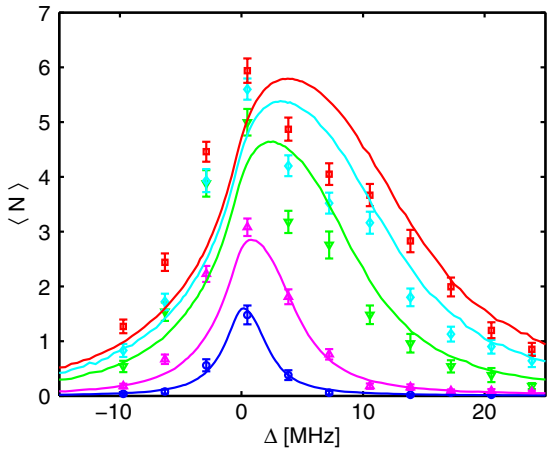

FIG. 2 (color online). Rydberg excitation spectra for different atomic densities: 5×10^{10} cm^{-3} (blue circles), 2×10^{11} cm^{-3} (cyan triangles), 8×10^{11} cm^{-3} (green triangles), 1.2×10^{12} cm^{-3} (magenta diamonds), and 1.5×10^{12} cm^{-3} (red squares). With increasing density we find enhanced excitation probabilities on the blue side of the resonance due to repulsive Rydberg-Rydberg interactions. The solid lines show the result of the rate equation model.

different atomic densities. At our lowest atomic densities (blue circles) the excitation spectrum is narrow and almost symmetric, reflecting the single-atom excitation probability. As the density is increased we observe a pronounced asymmetry extending to higher detunings, despite the fact that the single atom excitation probability is almost zero. This is consistent with the simple picture for the excitation of aggregates comprised of several nearby Rydberg atoms.

The mean number of Rydberg excitations only provides partial information on the underlying many-body correlations. Extending the analysis to higher order statistical moments (full counting statistics) one can obtain additional information. This is an established technique in quantum transport problems, e.g., whether electrons tunnel through a barrier as individual particles or in pairs [38]. To learn more about the excitation process we analyze the second-statistical moment quantified by the Mandel Q parameter, defined as $Q = \langle (N - \langle N \rangle)^2 \rangle / \langle N \rangle - 1$ where N is the number of excitations measured in a single run of the experiment. We also analyze the third moment characterized by $Q_3 = \langle (N - \langle N \rangle)^3 \rangle / \langle N \rangle - 1$. This quantity gives an additional measure of the correlations in our system and can be related to the three-body spatial correlation function $G_3(r_1, r_2, r_3)$ [20]. For uncorrelated excitation of single atoms we expect $Q = Q_3 = 0$ (Poissonian limit), and assuming independent excitation of m-atom aggregates $Q = m - 1$ and $Q_3 = m^2 - 1$, respectively (see Supplemental Material [33]). In the presence of correlations between aggregates the resulting possible Q and Q_3 would, depending on the degree of saturation, range from -1 to the values derived above. Estimating our statistical errors using bootstrap resampling [39], we conclude that measurements of fourth order and higher moments are not statistically significant for our sample sizes.

Figure 3(a) shows the measured Q parameter as a function of detuning at the highest density of 1.5×10^{12} cm^{-3}. The red diamonds show results averaged over 200 experimental realizations while the blue circles are based on 800 measurements per point. We observe a clearly asymmetric dependence of Q on the detuning. This is in marked contrast to recent observations involving Rydberg $|nD\rangle$ states featuring attractive as well as repulsive interactions, where large fluctuations were observed on either side of the resonance [14]. For negative detunings we measure $Q \approx 0$, which reflects Poissonian fluctuations in the limit of weak excitation. Around resonance we find Q factors clearly below 0, which indicate antibunching of excitations induced by the Rydberg blockade [8,14,15]. For $\Delta > 0$ the statistical distributions become super-Poissonian ($Q > 0$), which we attribute to the excitation of aggregates comprised of multiple Rydberg atoms. For Q_3 [Fig. 3(b)] we observe qualitatively similar behavior to Q, with $Q_3 \approx 0$ for $\Delta < 0$, suggesting independent (Poissonian) excitation of Rydberg atoms. For $\Delta > 0$ we find that Q_3 rapidly increases also indicating the presence of larger aggregates.

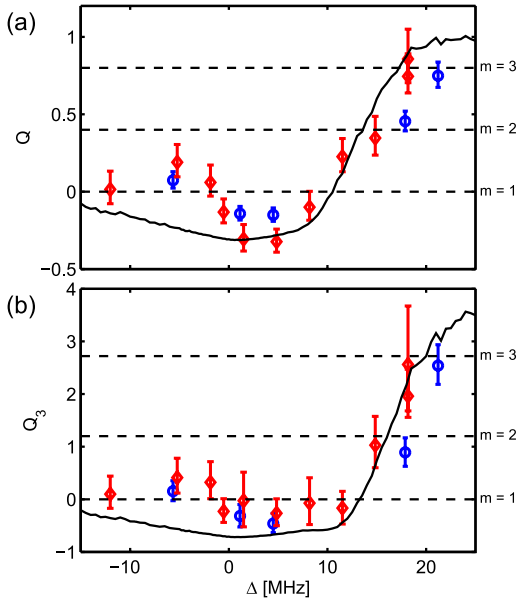

FIG. 3 (color online). Q (a) and Q_3 (b) as a function of the detuning Δ at a density of 1.5×10^{12} cm^{-3}. The red diamonds (blue circles) are extracted from a data set with 200 (800) experiments per data point. Error bars represent 68% confidence intervals determined via bootstrapping. The dashed lines indicate the expected Q and Q_3 factors corresponding to the excitation of exclusively single atoms, pairs, and triples. The solid lines show the statistical moments as obtained from the rate equation model.

The dashed horizontal lines in Fig. 3 show the simple scaling for m-atom aggregates, taking into account the finite detection efficiency (see Supplemental Material [33]). At large detunings ($\Delta \approx 20$ MHz) we find $Q \gtrsim 0.8$, consistent with an average aggregate size of $m \approx 3$ and a high probability that even larger aggregates are present. The data for $Q_3 \gtrsim 2.7$ are also consistent with $m \approx 3$, thereby providing independent confirmation for the aggregate size.

To address the question of how the aggregates form we estimate the dominant formation rates in the limit of large laser detuning. The overall rate for sequential excitation is limited by the off-resonant excitation rate of the first atom, $\gamma_1 \approx \Omega^2 \Gamma / (4\Delta^2)$, since subsequent excitation steps are resonant for the preferred distance $r = (C_6/\Delta)^{1/6}$. In comparison, if the total interaction energy for a state involving m excitations is precisely matched by the laser detuning, then simultaneous m-photon excitation can occur with a rate $\gamma_{m,\mathrm{sim}} = [\Omega^m / (2^{m-1} \prod_{i=1}^{m-1} \delta_i)]^2 / (m\Gamma)$, obtained by adiabatically eliminating all intermediate states. The detunings from the intermediate states involving $i < m$ excitations (assumed to be equidistantly spaced along a line) are $\delta_i = i\Delta - (i-1)m\Delta/(m-1)$. The ratio of sequential to simultaneous rates for m-atom aggregates therefore scales as $\Gamma^2 \Delta^{2m-4} \Omega^{2-2m}$. Accounting for the availability of atoms at specific distances leads to a slight modification of these rates, nonetheless, for $\Omega < \Delta$ the ratio still increases exponentially with aggregate size m. For our experimental parameters the rate for simultaneous $m = 2$-photon excitation is

approximately 1 order of magnitude smaller than sequential growth. For $m = 3$ simultaneous excitation is suppressed by an additional factor of $\approx 4 \times 10^3$ at $\Delta = 20$ MHz.

To further elucidate whether sequential excitation is the dominant formation mechanism in our experiments we perform time-dependent numerical simulations using an effective two-level rate equation (RE) model ([40], based on [32]). The RE approach can model our precise experimental geometry, but approximates many-body correlations via an energy shift depending on the state of the surrounding atoms. Thus it does not capture multiatom coherences which would be present in a simultaneous multiphoton excitation. Nonetheless, we find that the results of the RE model qualitatively reproduce the full statistical distributions including higher order moments for $\Delta > 0$ where the aggregates are formed [solid lines in Figs. 1(b), 2, and 3]. We observe a small discrepancy between theory and data on the red side of the resonance ($\Delta < 0$) and a slight shoulder in the mean number around $\Delta \approx 10$ MHz which cannot be explained by the RE model. This shoulder possibly indicates the presence of additional physical processes like atomic motion due to repulsive forces which would be more pronounced on the blue side of the resonance because of the excitation of Rydberg atoms with small separations. Nevertheless, given the good agreement, especially for the Mandel Q parameter in the regime $\Delta > 0$, we conclude that coherent multiphoton excitation is not required to explain our experimental findings, since such processes are not included in the RE treatment. Instead, for our parameters the dominant mechanism by which aggregates are formed at large detuning is via sequential (single-atom) excitations around an initial grain. This is further supported by time-dependent simulations which show that the off-resonant excitation of the initial grain is slow while the subsequent resonant excitation of additional atoms happens on faster time scales, as we show in the Supplemental Material [33].

To further substantiate that sequential excitation dominates over direct multiphoton excitation we benchmark the RE model with two-level wave function Monte Carlo (MCWF) simulations. The MCWF method includes multiatom coherences, but can only be applied to systems involving fewer excited atoms. Therefore, we simulate 50 atoms in a spherical volume with radius 2.285 μm and the other parameters being comparable to those of the experiments. The close agreement of the two simulations (see Fig. 1 in the Supplemental Material [33]), together with the good agreement between the RE model and experimental data is a strong indication for the sequential excitation indeed being the dominant process in our system.

Considering the good agreement between theory and experimental data, we can extract more information about the underlying many-body correlations from the results of the RE model. Specifically, we extract the second order spatial correlation function $G_2(r)$ (see Fig. 4), as defined in Ref. [40]. For $\Delta = +15$ MHz we observe strong liquidlike

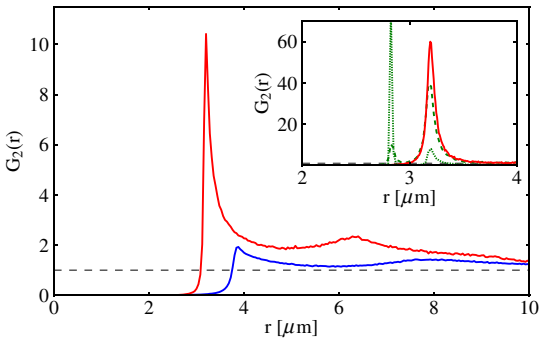

FIG. 4 (color online). Pair correlation functions $G_2(r)$ obtained from the RE model. The blue curve shows the correlation function for $\Delta = 5$ MHz, the red curve for $\Delta = 15$ MHz. The inset shows MCWF simulations for $\Delta = 15$ MHz, and dephasing rates $\Gamma = 0$ (green, dotted) and $\Gamma = 1$ MHz (green, dashed), compared to the RE simulation with $\Gamma = 1$ MHz (red, solid). To improve visibility, the dotted curve is scaled by a factor of $1/10$. The different peak amplitudes between the inset and main figure are due to the different simulation volumes and finite-size effects.

correlations [i.e., a strong first peak in $G_2(r)$ followed by peaks with decaying amplitudes], which are responsible for the large measured Q values. The pronounced peak at $r = (C_6/\Delta)^{1/6} \approx 3.2$ μm reflects a strongly preferred pair distance. A smaller peak at $r \approx 6.5$ μm is evidence for higher order correlations for $m > 2$. The peaks are strongly reduced for near resonant excitation ($\Delta = +5$ MHz). For resonant driving the peaks are even smaller, but still nontrivial correlations are present, as recently demonstrated experimentally [13]. These spatial correlations could be exploited in other areas of physics such as in the creation of strongly coupled plasmas [4,41,42]. Comparing to the $G_2(r)$ as obtained from MCWF simulations (100 atoms in a cylindrical volume with radius 1.65 μm and length 6 μm) we find again close agreement (Fig. 4, inset), apart from a small additional peak at $r = (C_6/2\Delta)^{1/6} \approx 2.8$ μm, which indicates a minor contribution from direct excitation of Rydberg atom pairs. This peak depends sensitively on the laser dephasing which quickly destroys multiatom coherences.

In conclusion, we have investigated laser excited Rydberg aggregates in a quasi-1D geometry. Using full counting statistics we determine their typical size as $m \gtrsim 3$. Our work emphasizes sequential excitation as the dominant mechanism under conditions of large dephasing. This highlights the need to account for dephasing and dissipation in theoretical descriptions of strongly correlated Rydberg gases. So far, most theoretical work has focused on lattice geometries [21,23,27–29]. It remains an open question whether results qualitatively different from ours are obtained for off-resonant excitation in optical lattices. However, even for lower dephasing rates, the vanishing multiphoton Rabi frequencies for large m suggests that sequential growth of aggregates is likely to play a significant role in existing experiments [13]. Distinguishing sequential and simultaneous excitation using FCS is

intrinsically challenging, since both processes lead to very similar results. Hence, in order to experimentally distinguish coherent multiphoton excitation versus sequential growth, future experiments could, e.g., measure the double peak structure in the spatial correlation function $G_2(r)$ as shown in Fig. 4 (inset).

We thank T. Pohl, O. Morsch, I. Bloch, M. Höning, and M. Fleischhauer for fruitful discussions. This work is supported in part by the Heidelberg Center for Quantum Dynamics, the Deutsche Forschungsgemeinschaft under WE2661/10.2, and the EU Initial Training Network COHERENCE. M. R. D. S. V. acknowledges support from the EU Marie-Curie program (Grant No. FP7-PEOPLE-2011-IEF-300870).

*whitlock@physi.uni-heidelberg.de
†Also at University of Science and Technology of China, Hefei, Anhui 230026, China.
weidemueller@uni-heidelberg.de

[1] S. Ichimaru, Rev. Mod. Phys. **54**, 1017 (1982).
[2] S. Sachdev, *Quantum Phase Transitions* (Cambridge University Press, Cambridge, England, 2001).
[3] E. Dagotto, Science **309**, 257 (2005).
[4] T. C. Killian, Science **316**, 705 (2007).
[5] I. Bloch, J. Dalibard, and W. Zwerger, Rev. Mod. Phys. **80**, 885 (2008).
[6] I. Carusotto and C. Ciuti, Rev. Mod. Phys. **85**, 299 (2013).
[7] D. Tong, S. M. Farooqi, J. Stanojevic, S. Krishnan, Y. P. Zhang, R. Côté, E. E. Eyler, and P. L. Gould, Phys. Rev. Lett. **93**, 063001 (2004); K. Singer, M. Reetz-Lamour, T. Amthor, L. G. Marcassa, and M. Weidemüller, *ibid.* **93**, 163001 (2004).
[8] A. Reinhard, K. C. Younge, and G. Raithel, Phys. Rev. A **78**, 060702 (2008).
[9] R. Löw, H. Weimer, U. Krohn, R. Heidemann, V. Bendkowsky, B. Butscher, H. P. Büchler, and T. Pfau, Phys. Rev. A **80**, 033422 (2009).
[10] T. Amthor, C. Giese, C. S. Hofmann, and M. Weidemüller, Phys. Rev. Lett. **104**, 013001 (2010).
[11] M. Viteau, M. G. Bason, J. Radogostowicz, N. Malossi, D. Ciampini, O. Morsch, and E. Arimondo, Phys. Rev. Lett. **107**, 060402 (2011).
[12] A. Schwarzkopf, R. E. Sapiro, and G. Raithel, Phys. Rev. Lett. **107**, 103001 (2011).
[13] P. Schauß, M. Cheneau, M. Endres, T. Fukuhara, S. Hild, A. Omran, T. Pohl, C. Gross, S. Kuhr, and I. Bloch, Nature (London) **491**, 87 (2012).
[14] M. Viteau, P. Huillery, M. G. Bason, N. Malossi, D. Ciampini, O. Morsch, E. Arimondo, D. Comparat, and P. Pillet, Phys. Rev. Lett. **109**, 053002 (2012).
[15] C. S. Hofmann, G. Günter, H. Schempp, M. Robert-de-Saint-Vincent, M. Gärttner, J. Evers, S. Whitlock, and M. Weidemüller, Phys. Rev. Lett. **110**, 203601 (2013).
[16] H. Weimer, R. Löw, T. Pfau, and H. P. Büchler, Phys. Rev. Lett. **101**, 250601 (2008).
[17] T. Pohl, E. Demler, and M. D. Lukin, Phys. Rev. Lett. **104**, 043002 (2010).
[18] J. Schachenmayer, I. Lesanovsky, A. Micheli, and A. J. Daley, New J. Phys. **12**, 103044 (2010).
[19] R. M. W. van Bijnen, S. Smit, K. A. H. van Leeuwen, E. J. D. Vredenbregt, and S. J. J. M. F. Kokkelmans, J. Phys. B **44**, 184008 (2011).
[20] C. Ates, T. Pohl, T. Pattard, and J. Rost, J. Phys. B **39**, L233 (2006).
[21] C. Ates and I. Lesanovsky, Phys. Rev. A **86**, 013408 (2012).
[22] D. Breyel, T. L. Schmidt, and A. Komnik, Phys. Rev. A **86**, 023405 (2012).
[23] M. Höning, D. Muth, D. Petrosyan, and M. Fleischhauer, Phys. Rev. A **87**, 023401 (2013).
[24] D. Petrosyan, M. Höning, and M. Fleischhauer, Phys. Rev. A **87**, 053414 (2013).
[25] F. Robicheaux and J. V. Hernández, Phys. Rev. A **72**, 063403 (2005).
[26] H. Weimer and H. P. Büchler, Phys. Rev. Lett. **105**, 230403 (2010).
[27] M. Mayle, W. Zeller, N. Tezak, and P. Schmelcher, Phys. Rev. A **84**, 010701 (2011).
[28] T. E. Lee, H. Häffner, and M. C. Cross, Phys. Rev. A **84**, 031402 (2011).
[29] M. Lemeshko, R. V. Krems, and H. Weimer, Phys. Rev. Lett. **109**, 035301 (2012).
[30] M. Gärttner, K. P. Heeg, T. Gasenzer, and J. Evers, Phys. Rev. A **88**, 043410 (2013).
[31] G. Günter, M. Robert-de-Saint-Vincent, H. Schempp, C. S. Hofmann, S. Whitlock, and M. Weidemüller, Phys. Rev. Lett. **108**, 013002 (2012).
[32] C. Ates, T. Pohl, T. Pattard, and J. M. Rost, Phys. Rev. Lett. **98**, 023002 (2007); Phys. Rev. A **76**, 013413 (2007).
[33] See Supplemental Material at http://link.aps.org/supplemental/10.1103/PhysRevLett.112.013002 for analysis of the statistical distributions including detection noise, benchmarking of the RE model, and further details on the aggregate formation mechanism.
[34] C. S. Hofmann, G. Günter, H. Schempp, N. M. L. Müller, A. Faber, H. Busche, M. Robert-de-Saint-Vincent, S. Whitlock, and M. Weidemüller, Front. Phys., doi: 10.1007/s11467-013-0396-7 (2013).
[35] D. Comparat and P. Pillet, J. Opt. Soc. Am. B **27**, A208 (2010).
[36] K. Singer, J. Stanojevic, M. Weidemüller, and R. Côté, J. Phys. B **38**, S295 (2005).
[37] R. Löw, H. Weimer, J. Nipper, J. B. Balewski, B. Butscher, H. P. Büchler, and T. Pfau, J. Phys. B **45**, 113001 (2012).
[38] Y. Nazarov and Y. Blanter, *Quantum Transport: Introduction to Nanoscience* (Cambridge University Press, Cambridge, England, 2009); X. Jehl, M. Sanquer, R. Calemczuk, and D. Mailly, Nature (London) **405**, 50 (2000); B. A. Muzykantskii and D. E. Khmelnitskii, Phys. Rev. B **50**, 3982 (1994).
[39] B. Efron, Ann. Stat. **7**, 1 (1979).
[40] K. P. Heeg, M. Gärttner, and J. Evers, Phys. Rev. A **86**, 063421 (2012).
[41] M. Robert-de-Saint-Vincent, C. S. Hofmann, H. Schempp, G. Günter, S. Whitlock, and M. Weidemüller, Phys. Rev. Lett. **110**, 045004 (2013).
[42] G. Bannasch, T. C. Killian, and T. Pohl, Phys. Rev. Lett. **110**, 253003 (2013).